Journal of Engineering Science and Technology
Vol. XX, No. Y (Year) PPP - QQQ

FABRICATION OF PRECAST CONCRETE SLAB PANELS INCORPORATING FOUNDRY SAND AND BLAST FURNACE SLAG AS A POTENTIAL WALL INSULATOR

A. SIVAKRISHNA[1], P. AWOYERA[2],*,
S. OSHIN[3], D. SUJI[3], R. GOBINATH[1]

[1]S R Engineering College, Warangal, India
[2]Department of Civil Engineering, Covenant University, Ota, Nigeria
[3]Department of Civil Engineering, P.S.G College of Technology, Peelamedu Coimbatore-6410 India
*Corresponding Author: paul.awoyera@covenantuniversity.edu.ng

Abstract

Increasing construction cost and environmental sustainability are persistent issues of concern in the built environment. Consequently, new generation materials are required for practical applications in order to considerably tackle the challenges. This work focused on the fabrication and testing of precast concrete slab panels produced using industrial by-products - foundry sand, as a partial replacement of fine aggregate, and ground granulated blast furnace slag as cement admixture. Foundry sand was substituted for manufactured sand in levels 0%, 10%, 20%, 30%, 40% and 50%, while granulated blast furnace slag (GGBS) was constantly added to cement at 30%, in a standard designed M40 concrete grade. The result showed that 40% of foundry sand was adequate for appreciable strength development in the modified mix. The same mixture was also found to have better insulation characteristics than the conventional mix. The wall panels tested in this study are quite economical when compared to competing building technologies.

Keywords: Blast furnace slag, Foundry sand, Precast concrete, Strength properties, Wall insulation.

1. Introduction

Environmental sustainability has been a major concern in the building and construction industry, mainly due to the persistent need to reduce materials and energy usage. A key focus has been the consumption of wastes emanating from industrial and construction activities into new projects. Thus, with numerous studies continually dwelling on the subject [1-7], some notable successes have been recorded.

River sand and sea sand, and manufactured sands are the conventional fine aggregates used for mortar and concrete production. However, the problems associated with the exploration of the sands, environmental degradation and depletion of the material sources, have birthed the idea to focus on other sources for materials. In like manner, Portland cement production involves the pollution of the environment with toxic compounds, which are deadly to human life. Therefore, in contribution to the concluded studies [8-10], the current study attempts to fabricate precast concrete slab panels incorporating foundry sand and blast furnace slag as ingredients, with a view to exploring both the strength and thermal conductivity of the concrete.

Studies [11-17], have shown that, granulated blast furnace slag (GGBS), a by-product generated from the production of steel, with or without chemical mixture, has cementitious properties that are suitable for concrete production. The application of GGBS cuts across several civil engineering material needs, such as in pavement construction [18, 19], concrete aggregate [20-22], and fillers for embankments [23]. Similarly, spent foundry sands, resulting from the foundry industry is another product that can fit application as aggregate. Thousands of tons of foundry sand are generated annually in some developing countries [24]. Five different foundry classes produce foundry sand. The ferrous foundries (gray iron, ductile iron, and steel) produce the common sand. While aluminium, copper, brass, and bronze produce yield other sands. About 3,000 foundries in India generate 6 million to 10 million tons of foundry sand per year. Although, there is repeated use of the sand within the foundry before its rejection as by-product, yet foundry sand reuse only covers about 10 percent elsewhere. The sands from the brass, bronze and copper foundries mostly end as wastes.

Spent sand is a non-hazardous product that has an economic benefit, yet not duly utilized for concrete production. In India, a large amounts of spent sand ends in local government landfills. There are many associated benefits with the reuse of foundry sand: minimal landfill tonnage or cost of disposal are some of the easily experienced.

Aside the routine investigations on the use waste materials as aggregate or binder in concrete, having the main target of reducing waste going to the landfills, there is a potential need for product development with the waste materials. Unfortunately, not much research outputs are available in this area. Thus, this study, not only considers wastes for replacement of conventional concrete constituents, but also explore the suitability of both GGBS and spent sand to improve strength and insulation characteristics of the concrete wall panel. In addition, the study attempts to develop a concrete mix design comprising both spent sand and slag for precast concrete elements.

2. Materials and Method

2.1. Materials

The materials used in this study include a grade 42.5 Ordinary Portland Cement (OPC) supplied by Shades & Co. Ltd., Coimbatore, India, and GGBS as binder, crushed rock as coarse aggregate, manufactured sand and foundry sand as fine aggregate, and potable water for concrete mixing. The physical properties of the cement were determined using IS 4031 [25]. Tables 1 and 2 present the physical properties and oxide composition of the cement used, respectively. There is a slight variation in specific gravities and standard consistencies of both cement and GGBS (Table 1). This suggests that the two binders can be blended together in cementitious mix, without altering the hydration and potential pozzolanic reactivity of the matrix [26]. In Table 2, the oxides composition of the cement showed that calcium oxide (CaO) is the most dominant (63 - 66%). This is a satisfactory property, because CaO is the catalyst that triggers hydration reaction in a cementitious mixture. Also, it can be seen from Table 2 that GGBS satisfy the requirement for a supplementary cementitious material (class C Fly ash), in that, $SiO_2 + Fe_2O_3 + Al_2O_3$ is greater than 70%, as described in ASTM C618 [27].

Table 1. Physical properties of cement.

Property	Cement	GGBS
Specific gravity	3.15	2.92
Standard consistency (%)	32	33
Setting time		
(i) Initial setting time (minutes)	345	-
(ii) Final setting time (minutes)	510	-
Fineness modulus	3%	-

Table 2. Chemical properties of binders.

Oxides	Composition (%)	
	Cement (by supplier)	GGBS
SiO_2	19 - 20	42.1
Fe_2O_3	3 - 3.5	1.2
Al_2O_3	6 - 6.2	9.4
CaO	63 - 66	36.4
Na_2O	0.1 - 0.12	1.9
LOI	1.5 - 1.75	3.1
K_2O	0.5 - 0.6	1.3
MgO	0.2 - 0.25	4.6

Table 3 shows the physical properties of the aggregate and Fig. 1 shows the SEM micrograph of foundry sand and GGBS. The SEM images were captured in the secondary electron mode. The aggregates possessed characteristics that satisfy the conditions for aggregates for concrete production in IS 2386 [28]. The SEM micrographs showed that foundry sand, Fig. 1(a) is sub-angular in shape, while GGBS, Fig. 1(b) have sharp particle edges. The angularity of the particles is adequate, because sharpness of particles can enhance the packing density of the matrix [29].

Table 3. Physical properties of aggregates.

Properties	Foundry sand	M-Sand	Crushed granite rock
Particle size (mm)	0.075 - 4.75		12.5 and down
Specific Gravity	2.38	2.54	2.85
Water absorption (%)	2.87	2.62	0.3
Fineness modulus	1.25	2.636	7.12
Particle shape	Sub angular		
Bulk density (Kg/m^3)			
(i) Loose state	1410	1537.96	
(ii) Rodded state	1571	1778.609	

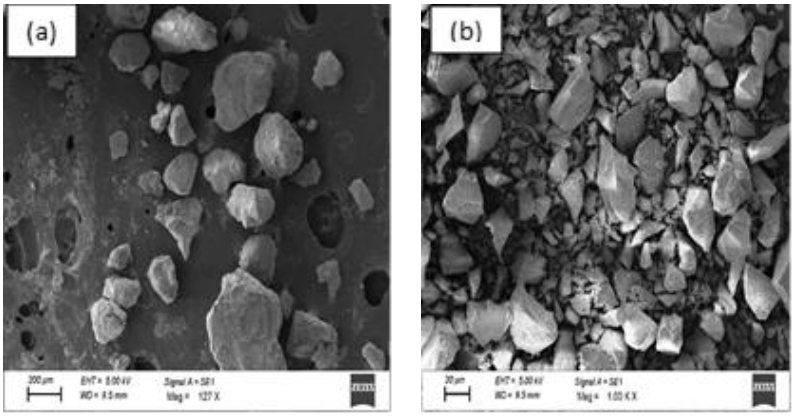

Fig. 1. SEM micrograph of (a) Foundry sand (127x) (b) GGBS (100x).

2.2. Mix proportions

This study adopted the standard procedures for design of an M40 grade of concrete in line with IS 10262 [30]. The mix proportion chosen was 1:1.89:3.0 with water/cement ratio of 0.47. Table 4 shows the full mix details for the tested samples. Mix CF1 represents the control, as it contains the conventional materials and constant addition of GGBS to cement. However, mixes CF2, CF3, CF4, CF5 and CF6 contain 10, 20, 30, 40 and 50% partial replacement of fine aggregate with foundry sands, respectively.

2.3. 2.3 Samples preparation and testing

For all the mixtures indicated in Table 4, the study initially performed preliminary tests covering evaluation of workability using slump, compressive strength of cubes (150×150×150 mm) and split tensile strength of cylinders (150×300 mm). Concrete testing was performed in accordance with the requirements of IS 516 [31].

Subsequently, the best mix that yielded higher cube and cylinder strength was selected for slab panel evaluation. From the code of practice for precast concrete construction [32], the standard size of the solid wall panel for this study are presented in Table 5.

Table 4. Mix proportion by weight.

Mix	Cement (kg/m^3)	GGBS (kg/m^3)	Fine Aggregate (kg/m^3)	Foundry sand (kg/m^3)	Water (L)	Coarse Aggregate (kg/m^3)
CF1	440	132	877.7	0	208	984.8
CF2	440	132	790.0	87.7	208	984.8
CF3	440	132	702.2	175.5	208	984.8
CF4	440	132	614.4	263.3	208	984.8
CF5	440	132	526.632	351.1	208	984.8
CF6	440	132	438.86	438.8	208	984.8

Table 5. Wall panel types and dimensions.

Wall type	Width (mm)	Height (mm)	Thickness (mm)
Square panel	1220 - 4572	1220 - 4572	270 - 350
Rectangular panel	1220 - 4572	2438.4 - 15240	270 - 350

However, this study adopted a scale-down model for casting the precast concrete panel. A description of the scale down model is in Table 6, while Fig. 2 shows the dimensions of the precast concrete wall panel.

Table 6. Size of precast concrete panel.

Sl. No.	Shape	Width (mm)	Height (mm)	Thickness (mm)
	Square:			
1.	(i) Standard	1220	1220	300
	(ii) Scale down model	300	300	75

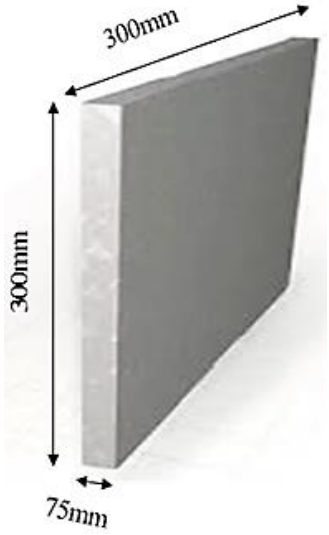

Fig. 2. Precast concrete wall panel.

Upon preliminary evaluation, mix CF5, having 40% foundry sand as a partial replacement of manufactured sand was found to produce higher strengths, somewhat like the conventional mix. Therefore, the production of slab panels in sizes 300 mm x 300 mm x 75 mm follows the mix CF5 materials proportion. The curing of slab panels followed immersion in water procedures for a period of 28 days, and the samples were prepared in a saturated surface dry condition prior to testing, by wiping out the surface moisture. Three samples were tested, and the average strength taken as the sample strength.

Figure 3 shows horizontally placed slab panel subjected to flexural resistance tests under four-point loading arrangement in the ultimate testing machine (UTM). Observation of the initial failure location showed that the failure location of all panels was within the middle third. This is based on the symmetry of the member, as mentioned in other study [33]. The machine also measured the stresses occurring at the failure zones within the slab.

The general expression used for flexural strength calculation is:

$$R = \frac{PL}{bd^2} \quad (1)$$

where R - Bending stress, P - Maximum applied load in N, L - Span length in mm, b - Average width of the specimen in mm, d - Average thickness of the specimen in mm

Fig. 3. Slab panel subjected to flexural strength test.

The thermal conductivity of the slab panels was determined using the Transient Plane Source (TPS) thermal conductivity system, which has the advantage of taking measurements relatively faster than other known methods. Figure 4 shows the set-up of the thermal conductivity test. The measurement of thermal conductivity followed the Fourier law of heat conduction. Under the principle, a planar heat source (sensor) in the form of a series of a concentric circular line, placed inside an infinite medium, generates a constant and stepwise heating power that diffuses into the sample under test. As a result, the mean temperature of the sensor rises over

time. Hence, the thermal conductivity calculation based on the measured temperature function of the sensor, is as follows:

$$Thermal\ Conductivity, k = \frac{P_o}{(\pi^{\frac{3}{2}} \times a \times Slope)} \quad (2)$$

where P_o is the heat liberation from the sensor in W, a - is the radius of the TPS sensor in a meter.

Thermal conductivity test requires using two identical concrete specimens of the same mix. Figure 4 shows a thermal conductivity system set-up adopted in this study. There is a hot disc (TPS Sensor) placed between the specimens, with a direct current power supplied to the specimen. Measurement of the sensor temperature took place at every 25 seconds, and the slope of the generated graph helps to calculate the thermal conductivity as indicated in Eq. (1).

Fig. 4. Thermal conductivity measurement system.

3. Results and Discussion

The workability of the concrete mixtures as obtained by slump test showed that the concrete mixtures possess true workability values, which are within the range of 60 to 85 mm. Figure 5 shows the strength comparison for all the tested concrete mixtures. The plot showed that both the compressive strength and split-tensile strength increased as the foundry sand substitution for manufactured sand increased up to 40%. However, replacement of foundry sand beyond 40% resulted in a reduction of the strength characteristics. Strength reduction as observed could be a function of less compatibility of materials in the matrix or significant increase in the free water of the mix, which is in excess than that required for hydration of cement paste and for proper compaction of fresh concrete.

Mixture CF5 gave the highest compressive strength and split-tensile strength, achieved at 40% substitution level of foundry sand. The best mix developed strength in excess of 7.62% than the reference concrete mix (having 0% foundry sand). Generally, the calculated strength properties were well within the permissible values. For design purposes, the split tensile strength is $0.45\sqrt{(fcu)}$, where fcu is the 28 days cube compressive strength.

Following the initial experimentation, which revealed that the replacement of M-sand by 40% of foundry sand gave the optimum percentage on comparison with

the conventional mix. The study consequently determined the compressive strength and flexural strength of precast concrete wall panels (300 mm x 300 mm x 75 mm) produced using the best mix. Figure 6 shows the wall panel subjected to compression loading. Figure 7 shows the compressive strength and flexural strength of selected wall panels.

The thermal conductivity of the selected concrete samples has been obtained using a power rating of 7 V, 2.05 A and 14.35 W. Figures 8 and 9 show the thermal conductivity of the control mix (CF1) and best mix (CF5), respectively. For CF1 mix, thermal conductivity was 1.428 W/m ^{0} C, and 1.288 W/m ^{0} C for CF5 mix. The results showed that sample CF5 possessed higher thermal conductivity than the conventional concrete (CF1). This can be a function of the moisture synergy in the matrix; because higher moisture in concrete is expected to reduce its thermal conductivity [34], because water has higher thermal conductivity than another medium [35]. The results suggest that CF5 mix could be useful for thermal insulation in buildings.

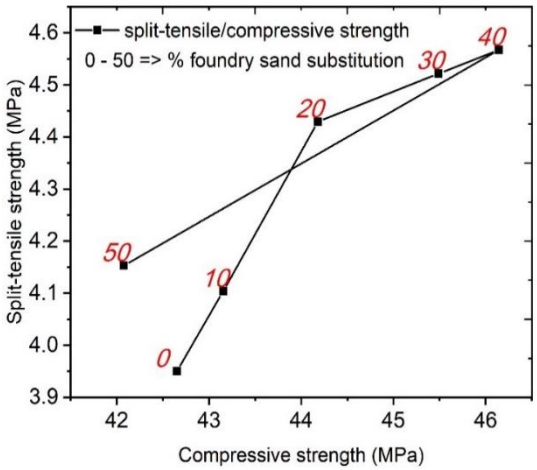

Fig. 5. Strength comparison for the concrete mixtures.

Fig. 6. Wall panel under compression test.

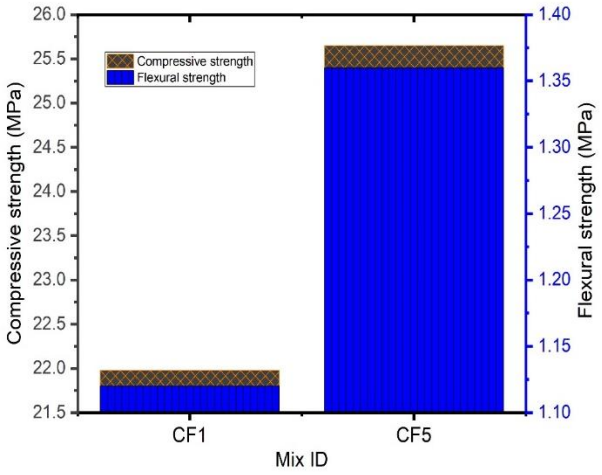

Fig. 7. Compressive strength and flexural strength of selected precast wall panels.

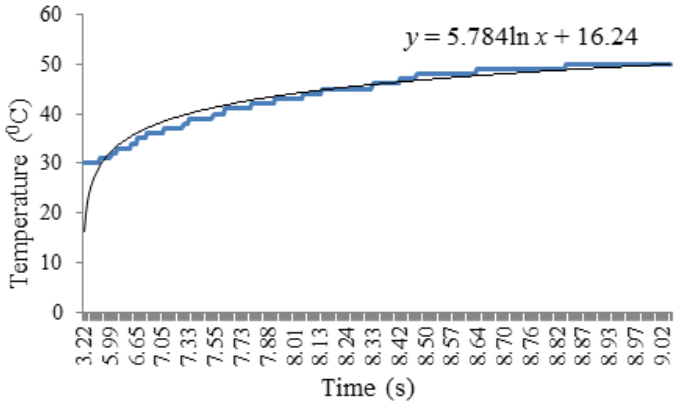

Fig. 8. Measured thermal conductivity in control concrete.

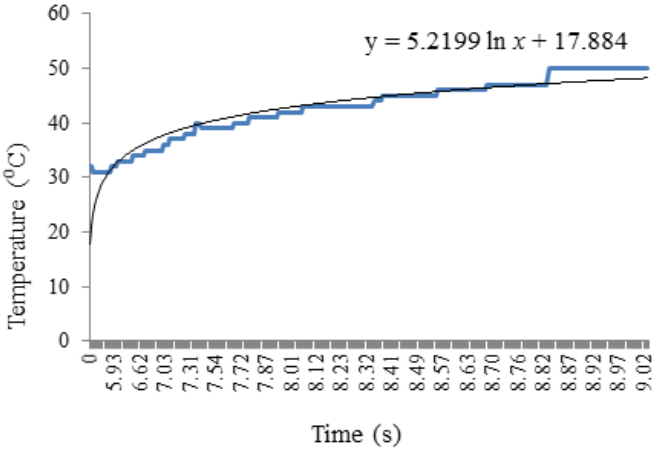

Fig. 9. Measured thermal conductivity in CF5 mix.

4. Conclusions

This study focuses on the fabrication of precast concrete slab panels incorporating foundry sand and blast furnace slag as a potential wall insulator. The conclusions drawn from the study are as follows:

- A preliminary investigation showed that replacement of manufactured sand by 40% of foundry sand gave most promising strength properties - in terms of compressive strength and split-tensile strength than the conventional mix.
- Strength increment in the modified concrete reflects the possibility of foundry sand acting as fill material that improves the compactness and reduces void in the concrete that in turn increase the strength characteristics. Although there was a reduction in strength, when foundry sand substitution increased beyond 40%, and this was traced to be associated with hydration of cement within the particles present in the concrete mix.
- Based on the investigations, it was clear that GGBS demonstrated good binding ability and contributes to the increased strength of the modified concrete mix, mostly when present in an optimum percentage of 30%.
- The compressive strength of the fabricated slab panel with 40% incorporation of foundry sand was optimal and the load carrying capacity increased to 14.3%.
- The flexural strength of 40% replaced foundry sand concrete panel (CF4) has an increase of 17.04% of flexural strength of panels compared to conventional mix panel.
- The study showed that a concrete mixture containing 40% foundry sand (CF5) possessed higher thermal conductivity than the control sample. Thus, higher value of thermal conductivity was attributed to be a function of the moisture synergy in the matrix, since foundry sand possess higher water absorption than manufacture sand.

Abbreviations

Al_2O_3	Aluminate
ASTM	American Standard Test Method
CaO	Calcium Oxide
Fe_2O_3	Ferrite
GGBS	Ground Granulated Blast-furnace Slag
IS	Indian Standard
K_2O	Potassium Oxide
LOI	Loss on Ignition
MgO	Magnesium Oxide
Na_2O	Sodium Oxide
SiO_2	Silica

References

1. Jin, R.; Yuan, H.; and Chen, Q. (2019). Science mapping approach to assisting the review of construction and demolition waste management research published between 2009 and 2018. *Resource, Conservation and Recycling*, 140, 175-188.

2. Sathanandam, T; Awoyera, P.O.; Vijayan, V.; and Sathishkumar, K. (2017). Low carbon building: Experimental insight on the use of fly ash and glass fibre for making geopolymer concrete. *Sustainable Environmental Research*, 27, 146-153.
3. Anandaraj, S.; Rooby, J.; Awoyera, P.O.; and Gobinath, R. (2019). Structural distress in glass fibre-reinforced concrete under loading and exposure to aggressive environments. *Construction and Building Materials*,197, 862-870.
4. Murth, P.; Awoyera, P.; Selvaraj, P.; Dharsana, D.; and Gobinath, R. (2018). Using silica mineral waste as aggregate in a green high strength concrete: workability, strength, failure mode, and morphology assessment. *Australian Journal Civil Engineering*, 16: 122-128.
5. Banu, S.; Chitra, G.; Gobinath, R.; Awoyera, P.; and Ashokkumar, E. (2018). Sustainable structural retrofitting of corroded concrete using basalt fibre composite. *Ecology, Environment and Conservation*, 24, 1384-1388.
6. de Brito, J.; Agrela, F.; and Silva, R.V. (2019). *Construction and demolition waste*. In: de Brito J, Agrela F (eds) New Trends in Eco-efficient and Recycled Concrete. Woodhead Publishing, United Kingdom.
7. Erdem, S.; Gürbüz, E.; and Uysal, M. (2018). Micro-mechanical analysis and X-ray computed tomography quantification of damage in concrete with industrial by-products and construction waste. *Journal of Cleaner Production*, 189, 933-940.
8. Balaguera, A.; Carvajal, G.I.; Albertí, J.; and Fullana-i-Palmer, P. (2018). Life cycle assessment of road construction alternative materials: A literature review. *Resource, Conservation and Recycling*, 132, 37-48.
9. Raji, M.; Nekhlaoui, S.; Hassani, I.; Essassi, E.; Essabir, H.; Rodrigue, D.; Bouhfid, R.; and Qaiss, A. K. (2019). Utilization of volcanic amorphous aluminosilicate rocks (perlite) as alternative materials in lightweight composites. *Composite Part B Engineering*, 165, 47-54.
10. Maddalena, R.; Roberts, J.J.; and Hamilton, A. (2018). Can Portland cement be replaced by low-carbon alternative materials? A study on the thermal properties and carbon emissions of innovative cements. *Journal of Cleaner Production*, 186, 933-942.
11. Liu, J.; Yu, Q.; Zuo, Z.; Yang, F.; Han, Z.; and Qin, Q. (2019). Reactivity and performance of dry granulation blast furnace slag cement. *Cement and Concrete Composite*, 95, 19-24.
12. Sekhar, D.C.; and Nayak, S. (2018). Utilization of granulated blast furnace slag and cement in the manufacture of compressed stabilized earth blocks. *Construction and Building Materials*, 166, 531-536.
13. Aliabdo, A.A.; Elmoaty, A.E.; and Emam, M.A. (2019). Factors affecting the mechanical properties of alkali activated ground granulated blast furnace slag concrete. *Construction and Building Materials*, 197, 339-355.
14. Mehta, A.; and Siddique, R. (2018). Sustainable geopolymer concrete using ground granulated blast furnace slag and rice husk ash: Strength and permeability properties. *Journal of Cleaner Production*, 205, 49-57.
15. Karthik, S.; Rao, P.; Awoyera, P.; Gobinath, R.; and Karri, R. (2018). Alkalinity and strength properties of concrete containing macro silica and ground granulated blast furnace slag. *IET Digital Library*, 4.

16. Karthika, V.; Awoyera, P.O.; Akinwumi, I.I.; Gobinath, R.; Gunasekaran, R.; Lokesh, N. (2018). Structural properties of lightweight self-compacting concrete made with pumice stone and mineral admixtures. *Romanian Journal of Materials*, 48, 208-213.
17. Karthik, S.; Rao, R.M.; Awoyera, P.; Akinwumi, I.; Karthikeyan, T.; Revathi, A.; Mathivanan, J.; and Manikandan, V. (2018). Beneficiated pozzolans as cement replacement in bamboo-reinforced concrete: the intrinsic characteristics. *Innovative Infrastructural Solutions*, 3, 50.
18. Phummiphan, I.; Horpibulsuk, S.; Rachan, R.; Arulrajah, A.; Shen, S.; and Chindaprasirt, P. (2018). High calcium fly ash geopolymer stabilized lateritic soil and granulated blast furnace slag blends as a pavement base material. *Journal of Hazardous Materials*, 341, 257-267.
19. Rudy, A.; Olek, J.; Nantung, T.; and Newell, R.M. (2009). *Statistical Optimization Of Low Slump Ternary Concrete Mixtures With Ground Granulated Blast Furnace Slag (GGBS) And High Calcium Fly Ash For Pavement Applications*. In: Brandt AM, Olek J (eds) Brittle Matrix Composites 9. Woodhead Publishing, Japan.
20. Netinger, I.; Bjegović, D.; and Vrhovac, G. (2011). Utilisation of steel slag as an aggregate in concrete. *Materials and Structures*, 44, 1565-1575.
21. Netinger, I.; Rukavina, M.J.; and Mladenovič, A. (2013). Improvement of Post-fire Properties of Concrete with Steel Slag Aggregate. *Procedia Engineering*, 62,745-753.
22. Awoyera, P.O.; Adekeye, A.W.; and Babalola, O.E. (2015). Influence of electric arc furnace (EAF) slag aggregate sizes on the workability and durability of concrete. *International Journal of Engineering and Technology*, 7(3), 1049-1056
23. Wang, G.C. (2016). *Case studies on slag utilization*. In: Wang GC (ed) The Utilization of Slag in Civil Infrastructure Construction. Woodhead Publishing, Korea.
24. de Barros, M. A.; Barros, R.M.; Silva, G.; and dos Santos, I.F.S. (2019). Study on waste foundry exhaust sand, WFES, as a partial substitute of fine aggregates in conventional concrete. *Sustainable Cities and Society*, 45,187-196.
25. Indian Standard. (1996). Methods of physical tests for hydraulic cement. *IS 4031*.
26. Awoyera, P.O.; Akinmusuru, J.O.; and Moncea, A (2017). Hydration mechanism and strength properties of recycled aggregate concrete made using ceramic blended cement. *Cogent Engineering*, 4.
27. ASTM International. (2008). Standard Specification for Coal Fly Ash and Raw or Calcined Natural Pozzolan for Use in Concrete. *ASTM C618*.
28. Indian Standard. (2002). Method of test for aggregate for concrete. *IS 2386*.
29. Awoyera, P.O.; Dawson, A.R.; Thom, N.H.; and Akinmusuru, J.O. Suitability of mortars produced using laterite and ceramic wastes: Mechanical and microscale analysis. *Construction and Building Materials*, 148, 195-203.
30. Indian Standard. (2009). Guidelines for concrete mix design proportioning. *IS 10262*.
31. Indian Standard. (1959). Method of Tests for Strength of Concrete. *IS 516*.

32. American Concrete Institute (ACI). (1993). Guide for Precast Concrete Wall Panels. *ACI 533R*.
33. Awoyera, P. (2016). Nonlinear Finite Element Analysis of Steel Fibre-reinforced Concrete Beam under Static Loading. *Journal of Engineering Science and Technology*, 11 (12), 1-9.
34. Wang, L.; Liu, P.; Jing, Q.; Liu, Y.; Wang, W.; Zhang, Y.; and Li, Z. (2018). Strength properties and thermal conductivity of concrete with the addition of expanded perlite filled with aerogel. *Construction and Building Materials*, 188, 747-757.
35. Asadi, I.; Shafigh, P.; Hassan, ZFBA.; and Mahyuddin, N.B. (2018). Thermal conductivity of concrete - A review. *Journal of Building Engineering*, 20, 81-93.